The American Journal of Pathology, Vol. 184, No. 5, May 2014

The American Journal of
PATHOLOGY
ajp.amjpathol.org

CARDIOVASCULAR, PULMONARY, AND RENAL PATHOLOGY

Identification of a Cell-of-Origin for Fibroblasts Comprising the Fibrotic Reticulum in Idiopathic Pulmonary Fibrosis

Hong Xia,* Vidya Bodempudi,* Alexey Benyumov,* Polla Hergert,* Damien Tank,* Jeremy Herrera,* Jeff Braziunas,† Ola Larsson,‡ Matthew Parker,* Daniel Rossi,* Karen Smith,* Mark Peterson,* Andrew Limper,§ Jose Jessurun,¶ John Connett,‖ David Ingbar,* Sem Phan,** Peter B. Bitterman,* and Craig A. Henke*

From the Departments of Medicine, Pharmacology,† and Laboratory Medicine and Pathology,¶ and the Division of Biostatistics School of Public Health,‖ University of Minnesota, Minneapolis, Minnesota; the Department of Oncology and Pathology,‡ Karolinska Institute, Stockholm, Sweden; the Department of Medicine,§ Mayo Clinic College of Medicine, Rochester, Minnesota; and the Department of Pathology,** University of Michigan Medical School, Ann Arbor, Michigan*

Accepted for publication January 2, 2014.

Address correspondence to Craig A. Henke, M.D., Box 276, University of Minnesota, 420 Delaware St SE, Minneapolis, MN 55455. E-mail: henke002@umn.edu.

Idiopathic pulmonary fibrosis (IPF) is a progressive disease of the middle aged and elderly with a prevalence of one million persons worldwide. The fibrosis spreads from affected alveoli into contiguous alveoli, creating a reticular network that leads to death by asphyxiation. Lung fibroblasts from patients with IPF have phenotypic hallmarks, distinguishing them from their normal counterparts: pathologically activated Akt signaling axis, increased collagen and α-smooth muscle actin expression, distinct gene expression profile, and ability to form fibrotic lesions in model organisms. Despite the centrality of these fibroblasts in disease pathogenesis, their origin remains uncertain. Here, we report the identification of cells in the lungs of patients with IPF with the properties of mesenchymal progenitors. In contrast to progenitors isolated from nonfibrotic lungs, IPF mesenchymal progenitor cells produce daughter cells manifesting the full spectrum of IPF hallmarks, including the ability to form fibrotic lesions in zebrafish embryos and mouse lungs, and a transcriptional profile reflecting these properties. Morphological analysis of IPF lung tissue revealed that mesenchymal progenitor cells and cells with the characteristics of their progeny comprised the fibrotic reticulum. These data establish that the lungs of patients with IPF contain pathological mesenchymal progenitor cells that are cells of origin for fibrosis-mediating fibroblasts. These fibrogenic mesenchymal progenitors and their progeny represent an unexplored target for novel therapies to interdict fibrosis. *(Am J Pathol 2014, 184: 1369–1383; http://dx.doi.org/10.1016/j.ajpath.2014.01.012)*

Progressive scarring of the heart, blood vessels, lung, liver, kidney, and brain is a leading cause of death worldwide.[1] Characteristic of these diseases, idiopathic pulmonary fibrosis (IPF) is a prevalent and progressive process.[2–6] In IPF, the fibroblast population expands within alveolar structures, resulting in scarred nonfunctional airspaces, progressive hypoxemia, and death by asphyxiation. As the disease process evolves, fibrosis spreads contiguously from affected alveoli into anatomically intact adjacent gas exchange units, resulting in an expanding reticular network of fibrotic tissue.[7–12] IPF lung fibroblasts display hallmarks that distinguish them from normal lung fibroblasts. Aberrant integrin signaling in the IPF fibroblast leads to sustained activation of proliferation and survival signaling pathways[13–15]; when grafted into model organisms, IPF fibroblasts form fibrotic lesions.[16,17] Despite their central role in

Supported by National Heart, Lung, and Blood Institute grants R01 HL074882 and P01 HL91775 (C.A.H.) and R01 HL089249 (P.B.B.); funds provided by the O'Brien family; the Swedish Research Council (O.L.); the National Center for Advancing Translational Sciences of the National Institutes of Health award 8UL1TR000114-02; and the Flow Cytometry Core Facility of the Masonic Cancer Center, a comprehensive cancer center designated by the National Cancer Institute, supported in part by P30 CA77598 and the University of Minnesota Imaging Center.

H.X. and V.B. contributed equally to this work.

Disclosures: None declared.

http://dx.doi.org/10.1016/j.ajpath.2014.01.012

mediating progressive fibrotic destruction of the lung, the origins of the IPF fibroblast are not known.

There is a well-established precedent for stem and progenitor cells as a source of the majority cell population in healthy and diseased organs. Normal lung tissue contains stem and progenitor cells that self-renew and give rise to transit-amplifying cells that maintain cell numbers in the steady state and mediate repair and regeneration in response to injury.[18–26] Neoplastic tissue contains pathological progenitors that exhibit self-renewal capacity and divide asymmetrically to produce malignant daughter cells[27–32]; disease-mediating progenitor cells have been implicated in chronic lung allograft rejection.[33,34]

Here, we report the identification of a subpopulation of cells in the lungs of patients with IPF with the properties of mesenchymal progenitors. Gene expression profiling of IPF lung mesenchymal progenitors distinguished them from mesenchymal progenitors isolated in a similar manner from the lungs of patient controls, with enrichment of genes associated with disease-relevant ontologies. The cellular progeny of IPF mesenchymal progenitors displayed all of the diagnostic hallmarks of the IPF fibroblast, including increased levels of phospho-Akt, increased expression of α-smooth muscle actin and type I collagen, and the ability to form fibrotic lesions in two model organisms. Analysis of IPF lung specimens revealed mesenchymal progenitor cells and cells bearing determinants of their progeny throughout the fibrotic reticulum. This is the first report in any progressive fibrotic disorder that documents diseased tissue harboring mesenchymal progenitor cells that are cells of origin for fibrosis-mediating fibroblasts.

Materials and Methods

Study Approval

De-identified patient samples were obtained under a waiver of informed consent from the University of Minnesota Institutional Review Board. Animal protocols were approved and conducted in accordance with the University of Minnesota Institutional Animal Care and Use Committee regulations.

Primary Mesenchymal Cell Lines

Eleven primary lung mesenchymal cell lines were established from patients who fulfilled diagnostic criteria for IPF, including a pathological diagnosis of usual interstitial pneumonia.[8] Patient controls were selected to be similar in age to patients with IPF with nonfibrotic lung disorders. On the basis of these criteria, we established 10 nonfibrotic primary control fibroblast lines from lung tissue uninvolved by the primary disease process: adenocarcinoma ($n = 4$), squamous cell carcinoma ($n = 1$), carcinoid tumor ($n = 2$), fibrosarcoma ($n = 1$), leiomyosarcoma ($n = 1$), or bronchiectasis ($n = 1$). Cell lines were derived from lungs, characterized as mesenchymal cells, and were cultivated as previously described.[35,36]

A significant challenge when studying primary cells from patient samples is the need for *ex vivo* preparation and *in vitro* expansion, procedures that introduce uncontrolled variables into the system. In addition, the relative difficulty of acquiring such samples prevents exact matching of demographic variables. To address these issues, standard technical variables (eg, subcultivation number, patient age, preparation batch) were tracked to minimize the bias they introduced into our results. Although this prevented introduction of systematic bias in our experiments, it does increase the measurement variance. Despite this, a principal components analysis (performed in R using the prcomp function) of the RNA-Seq data revealed the first principle component to partition the samples between mesenchymal progenitor cells and their progeny and the second principal component to partition the samples between IPF and control. We did not observe partitioning on the basis of any other technical variable we tracked. Although we cannot exclude the possibility that hidden technical confounders influenced the data, this analysis supports the robustness of our results.

Isolation of Mesenchymal Progenitor Cells

IPF and control mesenchymal progenitor cells were isolated from primary IPF and control mesenchymal cell cultures at passage 0 (initial isolate before subcultivation) through passage 4. To isolate progenitors, primary IPF and control mesenchymal cells were labeled with mouse anti–stage-specific embryonic antigen 4 (SSEA4) antibody conjugated to Alexa Fluor 647 and mouse anti-SSEA1 conjugated to phycoerythrin (BD Biosciences, San Jose, CA). Cells were sorted on a FACSAria Cell Sorter (BD Biosciences). Cells that were $SSEA4^+$ and $SSEA1^-$ (relative to mouse IgG3 κ isotype control conjugated to Alexa Fluor 647 and phycoerythrin) and <12 μm (designated small cells; forward and side calibrated using a 12-μm mesh; Millipore, Temecula, CA) were collected.

Multiparameter Flow Cytometry

Primary IPF and control mesenchymal cells were subjected to cell surface antigen phenotyping with the use of fluorescein isothiocyanate-, phycoerythrin-, or peridinin chlorophyll protein complex-cyanine 5.5–conjugated antibodies (BD Biosciences) against SSEA1, SSEA4, CD90, CD73, CD105, CD45, and CD34. Isotype-matched fluorophore-conjugated IgG antibodies were used as negative controls to set the gates. Cells were analyzed on a BD Biosciences FACSCalibur flow cytometer with the use of FlowJo Flow Cytometry Analysis software version 7.6.5 (TreeStar Inc, Ashland, OR).

Plastic-Adherent Clonal Growth Assay

Single-cell suspensions of $SSEA4^+$/$SSEA1^-$/small cells were sparsely plated on plastic tissue culture dishes and

maintained in Dulbecco's modified Eagle's medium (DMEM) + 10% fetal bovine serum (FBS; 37°C, 10% CO_2, 2 weeks). Enumeration of colony-forming unit fibroblast adherent colonies was performed microscopically after fixing cells with methanol and staining with crystal violet.

Tri-Lineage Differentiation Assay

IPF and control SSEA4$^+$/SSEA1$^-$/small cells were analyzed for tri-lineage differentiation capacity by using the following assay kits: StemPro Osteogenesis Differentiation Kit, catalog number A10072-01; Adipogenesis Differentiation Kit, catalog number A10070-01; Chondrogenesis Differentiation Kit, catalog number A10071-01; Gibco, Grand Island, NY). After 21 days in differentiation culture conditions, cells were fixed and labeled with antibodies against fatty acid binding protein 4 (adipocytes), osteocalcin (osteocytes), or aggrecan (chondrocytes) and visualized by immunofluorescence (all antibodies from R&D Systems, Minneapolis, MN).

RT-PCR

RT-PCR was performed as previously described.[36] PCR reactions were subjected to gel electrophoresis, and only primers yielding a single product of the appropriate length were used. We took special care to validate octamer-binding transcription factor 4 (Oct4A) because of our intent to use it for immunohistochemical lung tissue analysis. This included using primer sequences documented to be specific[37] and sequence-verifying the gel-purified PCR product.

Western Blot Analysis

Blots were performed as previously described.[13–15]

Derivation of Progeny from Mesenchymal Progenitor Cells

IPF and control progeny (ie, daughter cells) were derived from SSEA4$^+$/SSEA1$^-$/small cells that had undergone fluorescence-activated cell sorting (FACS).

Progeny from a Population of Flow-Sorted Progenitor Cells

IPF and control progenitors were isolated from IPF and control primary mesenchymal cell cultures by flow cytometry that selected for SSEA4^{hi}/SSEA1$^-$/small cells. One hundred progenitors were placed into 3.8-cm^2 wells of 12-well tissue culture clusters and allowed to propagate and differentiate under tightly standardized conditions (DMEM + 10% FBS, 37°C, 10% CO_2) for 21 days. The resultant cell population was designated IPF or control progeny.

Progeny from a Single IPF or Control Mesenchymal Progenitor Cell

Individual SSEA4$^+$/SSEA1$^-$/small cells (98.88% pure by postsort analysis) that had undergone FACS from a primary IPF and control mesenchymal cell culture (subcultivation 1) were placed at a concentration of one cell per well into 96-well clusters coated with STEMPRO MSC SFM CTS (Gibco) that contained 2.5% methylcellulose. Cultures were continued (DMEM + 10% FBS, 37°C, 10% CO_2, 14 days) until a small number of colonies formed. The two largest IPF colonies and four largest control colonies were transferred to separate tissue culture dishes (35 mm) and allowed to propagate and differentiate (DMEM + 20% FBS, 37°C, 10% CO_2) for 21 days.

Immunohistochemistry

Immunohistochemistry was performed on 4-μm paraffin-embedded IPF and control lung tissue and mounted on polylysine-coated slides. The sections were deparaffinized in xylene, rehydrated through a graded methanol series, quenched with 0.3% hydrogen peroxide in methanol, and immersed in a 98°C water bath for 30 minutes in Citrate Buffer (pH 6.0) for antigen retrieval. Sections were placed in 5% normal horse serum (Jackson ImmunoResearch Laboratories, West Grove, PA) to block nonspecific binding of secondary antibodies. Endogenous avidin and biotin binding sites were blocked by sequential incubation for 15 minutes each with an Avidin/Biotin Blocking Kit (Vector Laboratories, Burlingame, CA) and incubated overnight (18 to 20 hours, 4°C) in the monoclonal human primary antibodies, Oct4 clone 10H11·2 (1:500; Millipore), SSEA-4 (1:100; Abcam, Cambridge, MA), and α-smooth muscle actin (α-SMA; 1:100; Vector Laboratories). Sections were rinsed with PBS, placed in biotinylated horse anti-mouse IgG secondary antibody (1:500) for 30 minutes at room temperature, followed by R.T.U. Horseradish Peroxidase Streptavidin Complex (Vector Laboratories) for 30 minutes. Specific antibody binding was detected by using a 3,3′ diaminobenzidine peroxidase kit (DAB; Vector Laboratories). For double antigen labeling, we followed the protocol described above in a sequential manner with two modifications: the reagent used to prevent nonspecific binding was 5% normal horse serum/5% normal goat serum in a 1:1 ratio solution for the second antibody, and DAB/Ni was used as the detection reagent. All sections were counterstained with hematoxylin (Invitrogen, Frederick, MD) for 2 minutes, and PBS was applied to blue for 30 minutes. Specimens were coverslipped with a Prolong Antifade Kit (Invitrogen/Molecular Probes) and stored overnight at room temperature without light before image analysis.

In Vivo Fibrogenesis Assays

Zebrafish Xenotransplantation

Cells stained with a vital dye [either 5 μmol/L carboxyfluorescein succinimidyl ester (CFSE) or PKH26 (Sigma-Aldrich, St. Louis, MO)] were grafted into the central portion of the zebrafish embryo blastoderm at the oblongsphere stages as previously described.[16] Embryos were

immobilized with Tricane after 48 hours. Fluorescent and corresponding bright field imaging of the CFSE-stained grafts in live embryos were performed with a Zeiss Axiovert upright microscope (Carl Zeiss, Thornwood, NY). After image acquisition, embryos were fixed with 4% paraformaldehyde, infiltrated with increasing concentrations of sucrose/PBS, and cryoembedded in OCT. For immunostaining, 5-μm sections were fixed in 100% methanol, rinsed in PBS, blocked with normal donkey serum, and incubated with the appropriate primary antibody. To identify engrafted human cells in zebrafish embryos, sections were incubated with CD59 [MEM-43] mouse monoclonal antibody (1:500; Abcam), followed by donkey anti-mouse cyanine 3 (1:500; Jackson ImmunoResearch Laboratories). Collagen type I was identified with human anti-procollagen type I antibody (1:200; Abcam) conjugated with horseradish peroxidase, and counterstained with H&E. The size of the fibrotic reticulum was quantified as previously described.[16]

Adoptive Transfer into Immunodeficient Mice

Cells were suspended in PBS (10^6 cells/mL) and injected via the tail vein into nonobese diabetic/severe combined immunodeficient/IL-2 receptor γ/β_2 microglobulin mice (The Jackson Laboratory, Bar Harbor, ME) according to a published protocol.[17] Mice were euthanized 60 days after adoptive transfer of human cells. Histological analysis of lung tissue was performed on paraffin-embedded and frozen lung tissue after H&E and trichrome staining. Cells positive for human β_2-microglobulin by immunohistochemistry (anti-human β_2 microglobulin antibody; Santa Cruz Biotechnology, Inc., Santa Cruz, CA) were identified as human. The presence of lung fibrotic lesions by histological analysis served as the primary end point.[17]

Transcriptional Profiling and Analysis of RNA Sequencing Data

RNA was isolated from freshly sorted SSEA4$^+$/SSEA1$^-$/small cells or their progeny (IPF and control, $n = 4$; ie, 16 samples total) and sequenced (50-bp paired-end read run) on an Illumina Hiseq 2000. Sequence reads were aligned to hg19 with Tophat 2.0.8 (Bowtie 2.1.0.0, allowing one mismatch). Only reads that aligned uniquely were kept. Counts were mapped to genes by using the R package GenomicRanges (Aboyoun, no date). The count data were log2 transformed and normalized with quantile normalization. Differential expression was identified with the random variance model modified *t*-test.[38] We used GAGE version 2.8.0[39] and annotation from the Gene Ontology Consortium[40] to identify enriched cellular processes. Input data were signed (direction of regulation) −log10 (random variance model *P* values).

Validity testing was conducted by real-time quantitative PCR (qPCR) as previously described.[41] The four genes chosen (*FLT1, MAP3K8, IGF2BP1, YBX1*) were selected from the 117 genes that met the following two criteria: they were assigned to the most significant ontologies that distinguished IPF from control, and among all genes that were altered ($P < 0.05$) in both IPF mesenchymal progenitors and IPF progeny relative to their control counterparts, the genes chosen displayed co-regulation between IPF mesenchymal progenitor cells and their progeny (ie, up in both progenitors and progeny or down in both progenitors and progeny). Total RNA was isolated and reverse transcribed by using a Taqman Reverse Transcriptase Reagent Kit (Roche, Indianapolis, IN) and primed with random hexamers. Primer sequences for selected genes were selected by using National Center for Biotechnology Information (NCBI) Primer-BLAST. qPCR was performed with a LightCycler FastStart DNA Master^{PLUS} SYBR Green I Kit (Roche). Primer sequences were as follows: FLT1, 5′-ACCAAAGCAATTCCCATGCC-3′ (forward), 5′-CAGCTACGGTTTCAAGCACC-3′ (reverse); MAP3K8, 5′-GCTTCCCTGGAGAGAAACCC-3′ (forward), 5′-ATTCCTCGGTGCTTCCTGTG-3′ (reverse); IGF2BP1, 5′-ACCTCCATTTACGGCCTCTTT-3′ (forward), 5′-TCTCCCCATTTTCCCCTCTTC-3′ (reverse); and YBX1, 5′-TCATCGCAACGAAGGTTTTGG-3′ (forward), 5′-GCCTTGAACTGGAACACCAC-3′ (reverse).

Samples were quantified at the log-linear portion of the curve by using LightCycler analysis software version 3.5 and compared with an external calibration standard curve.

Data Analysis

For zebrafish data, IPF was represented as an indicator variable (0 for controls, 1 for patients with IPF). A repeated measures analysis of variance was used to compare cells from patients with IPF with cells of controls, with the length of migration as the outcome variable, IPF as the variable of interest, and an interaction term for IPF with embryo. For the mouse data, fibrosis was coded as 0 (absent) or 1 (present), and the relationship between IPF and fibrosis was evaluated with Fisher exact test. Quantitative data are expressed as means ± SD. $P < 0.05$ was considered significant. Principal components analysis was performed in R by using the prcomp function.

Results

Mesenchymal Progenitor Cells Can Be Isolated from the Lungs of Patients with IPF

We established primary mesenchymal cell lines from IPF and control lung tissue.[35] From these primary cell lines, we isolated mesenchymal progenitors by FACS on the basis of expression of SSEA4,[42] lack of SSEA1, and size (<12 μm) (Figure 1A). No consistent differences were found in yields of SSEA4$^+$ cells from IPF or control primary mesenchymal cell lines. To characterize the SSEA4$^+$/SSEA1$^-$/small cell population, we tested for signature mesenchymal stem/stromal cell (MSC) determinants.[43,44] Similar to MSCs, control

and IPF SSEA4$^+$/SSEA1$^-$/small cells expressed CD73, CD90, and CD105; both lacked expression of the fibrocyte determinants CD34 and CD45 (Figure 1B); both expressed vimentin (Figure 1C); and both were negative for the hematopoetic cell determinants CD11, CD19, and human leukocyte antigen DR (data not shown). One defining property of MSCs is the ability of a single precursor cell, termed a colony-forming unit fibroblast, to generate plastic-adherent colonies.[45] Both IPF and control SSEA4$^+$/SSEA1$^-$/small cells displayed this property (Figure 1D). In common with MSCs, both IPF and control SSEA4$^+$/SSEA1$^-$/small cells exhibited tri-lineage mesenchymal differentiation capacity (Figure 1E); expressed mRNA encoding the progenitor transcription factors Oct4A, sex determining region Y (SRY)-box 2 (Sox2), and Nanog (Figure 1F); both expressed active β-catenin; and neither expressed Kruppel-like factor 4 (data not shown). Thus, our studies indicate that primary mesenchymal cell cultures derived from IPF and control lungs contain mesenchymal progenitor cells that share properties with MSCs.

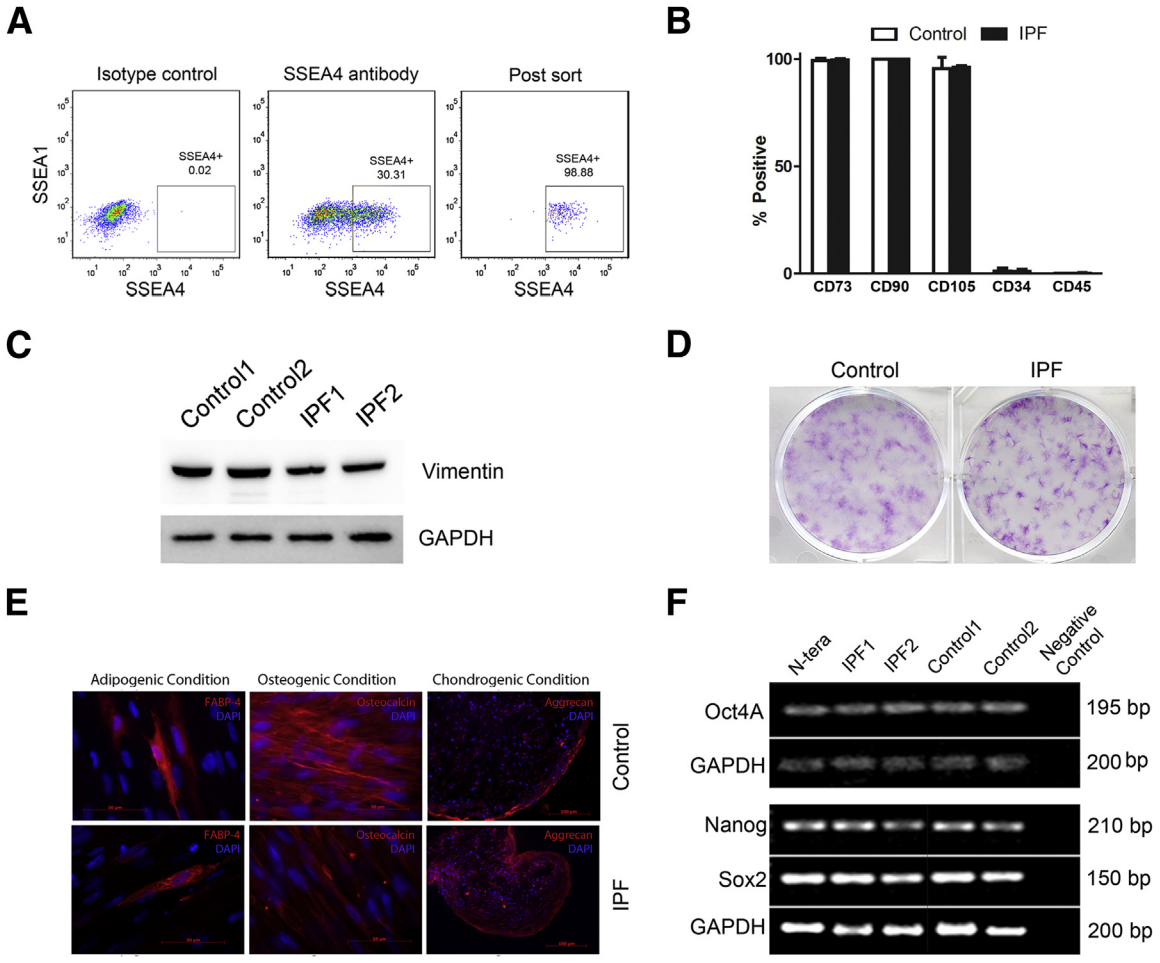

Figure 1 Recovery and characterization of SSEA4$^+$/SSEA1$^-$/small cells from IPF and control primary mesenchymal cell lines. **A:** Representative of SSEA4$^+$/SSEA1$^-$/small cells that had undergone FACS. Primary mesenchymal cell lines were sorted by FACS to isolate cells with relatively high surface expression of SSEA4 and low surface expression of SSEA1. Shown are the gates used (**solid lines**) to define the SSEA4$^+$/SSEA1$^-$ cell population. The **boxed area** indicates the region defined as SSEA4$^+$/SSEA4$^-$. Cells were also sorted on the basis of size (forward and side scatter were calibrated with cells passing through a 12-μm mesh). **B:** Flow cytometric analysis of SSEA4$^+$/SSEA1$^-$/small cells for expression of cell surface determinants used to define MSCs (CD73, CD90, CD105) and fibrocytes (CD34 and CD45). Data shown are from SSEA4$^+$/SSEA1$^-$/small cells from two control and two IPF primary mesenchymal cell lines (means ± SD). **C:** SSEA$^+$/SSEA1$^-$/small cells were examined for vimentin expression by Western blot analysis. GAPDH is shown as a loading control. **D:** Colony-forming unit fibroblast assay: SSEA4$^+$/SSEA1$^-$/small cells were seeded at clonal density onto plastic tissue culture dishes (500 cells/9.5 cm^2) and maintained in culture for 14 days. Shown are representative images of crystal violet-stained colonies formed by SSEA4$^+$/SSEA1$^-$/small cells sorted from two control and two IPF primary mesenchymal cell lines, each assayed in triplicate. **E:** SSEA4$^+$/SSEA1$^-$/small cells were investigated for tri-lineage differentiation capacity: i) adipocytes as determined by immunoreactivity to anti-FABP4 and the presence of lipid within the cells; ii) osteocytes by immunoreactivity to anti-osteocalcin; and iii) chondrocytes, as determined by the presence of aggrecan. Data shown are representative of SSEA4$^+$/SSEA1$^-$/small cells sorted from three control and three IPF primary mesenchymal cell lines. **F:** RT-PCR analysis of IPF and control SSEA4$^+$/SSEA1$^-$/small cells for progenitor transcription factors: Oct4A, Nanog, and Sox2, with GAPDH serving as a loading control. Human testicular embryonal carcinoma cells (N-TERA) were used as a positive control and PCR with primers but no cDNA as a negative control. Data shown are representative of SSEA4$^+$/SSEA1$^-$/small cells sorted from four IPF and four control primary mesenchymal cell lines. The Oct4A band was sequenced from one IPF and one control to verify its identity. Scale bars: 50 μm (**E**, **left** and **middle panels**); 100 μm (**E**, **right panels**). FABP4, fatty acid binding protein 4; GAPDH, glyceraldehyde-3-phosphate dehydrogenase.

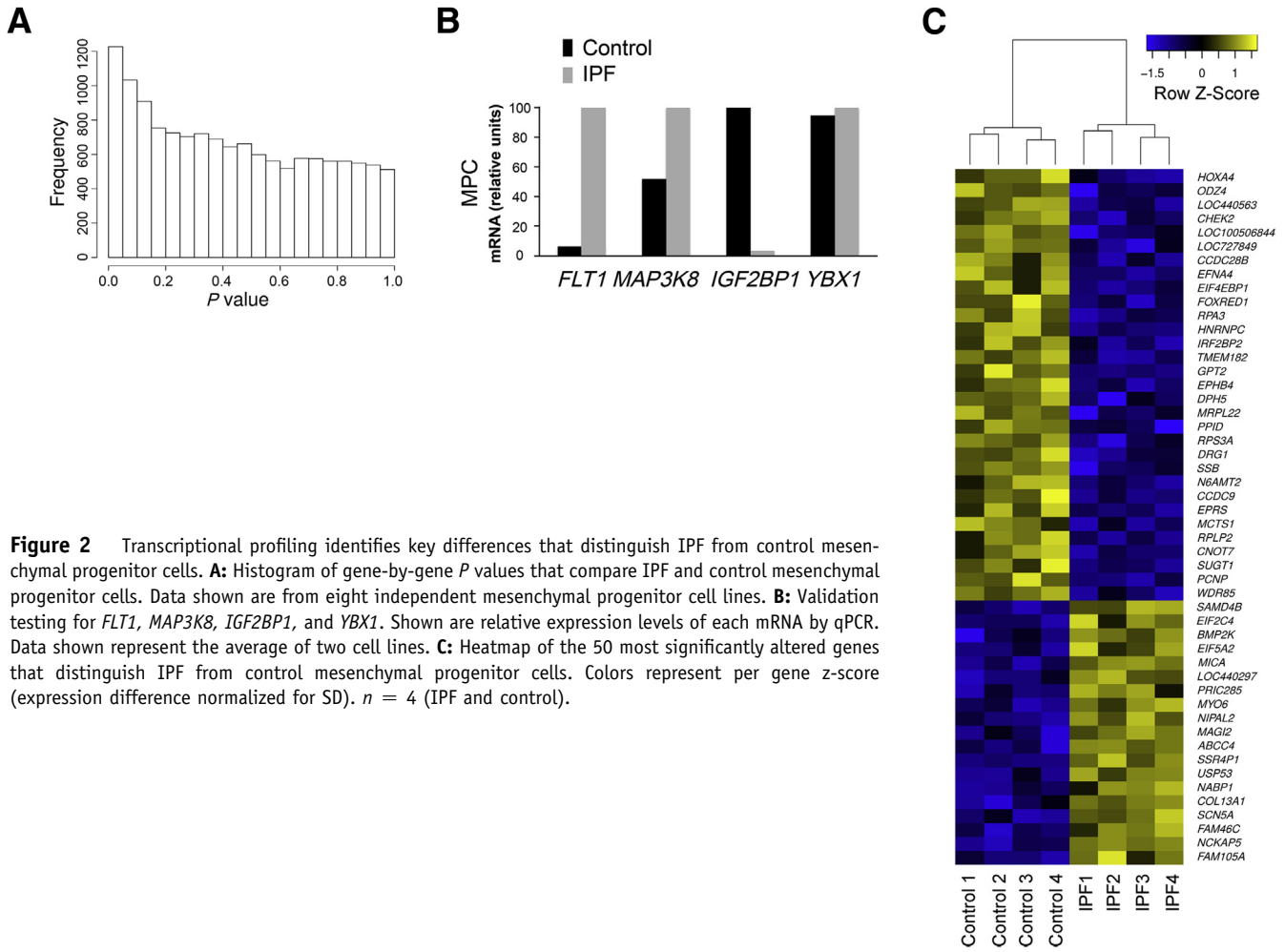

Figure 2 Transcriptional profiling identifies key differences that distinguish IPF from control mesenchymal progenitor cells. **A:** Histogram of gene-by-gene *P* values that compare IPF and control mesenchymal progenitor cells. Data shown are from eight independent mesenchymal progenitor cell lines. **B:** Validation testing for *FLT1, MAP3K8, IGF2BP1,* and *YBX1*. Shown are relative expression levels of each mRNA by qPCR. Data shown represent the average of two cell lines. **C:** Heatmap of the 50 most significantly altered genes that distinguish IPF from control mesenchymal progenitor cells. Colors represent per gene z-score (expression difference normalized for SD). $n = 4$ (IPF and control).

Transcriptional Profiling Identifies Key Differences That Distinguish IPF from Control Mesenchymal Progenitor Cells

To elucidate molecular processes that distinguish control and IPF mesenchymal progenitor cells, we defined steady state mRNA levels genomewide. There were significant differences in gene expression between IPF and control mesenchymal progenitor cells on the basis of enrichment of genes with low *P* values (Figure 2A). A heatmap of the 50 most significant genes ($P < 0.002$) revealed a distinct IPF molecular signature (Figure 2C). To identify significant differences in disease-relevant functions, we conducted a gene set enrichment analysis.[39,40] IPF mesenchymal progenitor cells displayed significant differences from controls in several disease-relevant ontologies, with a large number of gene ontology terms related to control of gene expression and proliferation (Supplemental Table S1). To test the validity of our transcriptional profiling, we directly quantified four genes that differed between IPF and control mesenchymal progenitor cells (for detailed selection criteria, see *Materials and Methods*): *FLT1* and *MAP3K8* (both genes showed elevated expression in IPF mesenchymal progenitors) and *YBX1* and *IGF2BP1* (both genes showed elevated expression in control mesenchymal progenitors). qPCR validated the transcriptional profiling for three of four genes (*FLT1, MAP3K8, IGF2BP1*), with *YBX1* showing no significant difference (Figure 2B). Thus, IPF mesenchymal progenitors display a pattern of gene expression that distinguishes them from their control counterparts.

IPF Mesenchymal Progenitor Cells Are Cells of Origin for IPF Fibroblasts

IPF lung fibroblasts have phenotypic hallmarks that distinguish them from controls.[13–15,46] They express higher levels of α-SMA and type I collagen, express lower levels of caveolin-1 and phosphatase and tensin homologue (PTEN), and manifest pathological activation of the phosphatidylinositol 3-kinase/Akt signaling pathway, resulting in aberrantly high levels of phospho-Akt. To analyze the daughter cells of mesenchymal progenitors for these hallmarks, we used FACS to sort $SSEA4^{+}/SSEA1^{-}$/small cells from IPF and control primary mesenchymal cell cultures and allowed them to propagate and differentiate under tightly standardized conditions (Supplemental Figure S1). Prior work

indicates that as mesenchymal progenitors propagate and differentiate *in vitro*, they display typical fibroblast morphology and lose expression of SSEA4, and Oct4 relocates from the nucleus to the cytoplasm where it persists for a period of time before being degraded.[47] In accord with this, irrespective of origin, the progeny of mesenchymal progenitors displayed typical fibroblast morphology and lost SSEA4 expression (representative examples shown in Figure 3A); and Oct4 transited from the nucleus to the cytoplasm in IPF progeny and was at the limit of detection in controls (Figure 3B). However, only the daughter cells of IPF mesenchymal progenitors displayed IPF fibroblast hallmarks: increased levels of α-SMA, type I collagen, and phospho-Akt and decreased levels of PTEN and caveolin-1 (Figure 3, C and D). These data showthat IPF mesenchymal progenitors produce SSEA4$^-$/nuclear Oct4$^-$/cytoplasmic Oct4$^+$ daughter cells with the biochemical hallmarks of IPF fibroblasts.

When grafted into developing zebrafish embryos or immunocompromised mice, only IPF fibroblasts form fibrotic lesions.[16,17] As a test of their fibrogenic potential, we examined whether IPF mesenchymal cell progenitors or their progeny displayed this behavior in both model organisms. Numerous studies have indicate that stem/progenitor cells integrate into the tissues of developing embryos after xenogenic transplantation.[48–54] Consistently, we found that normal human bone marrow MSCs, when injected into the developing zebrafish, formed multiple small grafts that were incorporated into anatomically normal-appearing tissues and did not disrupt development. Similar to bone marrow MSCs, both IPF and control mesenchymal progenitors incorporated into the developing tissues of phenotypically normal embryos (Supplemental Figure S2). In sharp contrast, the properties of the mesenchymal progenitor progeny depended on their origin. Control progeny formed a small mass of nonmotile cells in the zebrafish, whereas IPF progeny formed an extensive fibrotic reticulum (Table 1, Figure 3, E–G, and Supplemental Figure S3, A and B) and expressed human procollagen type I (Supplemental Figure S3C). Results in the mouse assay paralleled results in the zebrafish, with the outcome depending on the origin of the mesenchymal progenitor progeny. The lungs of mice receiving the progeny of control mesenchymal progenitors were anatomically normal; whereas fibrotic lung lesions formed in all mice receiving the daughter cells of IPF progenitors ($P < 0.0022$) (Table 2, Figure 3H, and Supplemental Figure S4). Thus, only the progeny of IPF mesenchymal progenitors form fibrotic lesions *in vivo*—a defining hallmark of the IPF fibroblast.

Although FACS efficiently isolates a nearly pure population of SSEA4$^+$/SSEA1$^-$/small cells (>98% pure), if even a small minority subpopulation included differentiated primary fibroblasts that had a proliferative advantage, after 21 days in culture these cells rather than the progeny of SSEA4$^+$/SSEA1$^-$/small cells could be the dominant cell type. To test for this possibility, we labeled the SSEA4$^+$/SSEA1$^-$/small cell population that had undergone FACS with CSFE, a vital dye that covalently binds to intracellular proteins and is stoichiometrically diluted as cells divide. When we quantified dye intensity during a 6-day interval, we observed a single, uniform pattern of CFSE dilution characteristic of a uniformly proliferating population (Supplemental Figure S5). This result excluded the possibility that the progeny of SSEA4$^+$/SSEA1$^-$/small cells were contaminated by a rapidly proliferating subpopulation of differentiated IPF fibroblasts.

As direct proof of concept, we generated daughter cells from a single FACS-sorted IPF mesenchymal progenitor cell (Figure 4A). When analyzed for IPF fibroblast hallmarks, the clonal progeny of a single IPF progenitor cell displayed increased levels of α-SMA and type I collagen, low levels of caveolin 1 and PTEN accompanied by increased levels of phospho-Akt (Figure 4B), and formed an extensive fibrotic reticulum in the zebrafish assay (Figure 4, C and D, and Supplemental Table S2). Interestingly, the cell population resulting from a single control progenitor cell was much smaller than the population from an identically cultured single IPF progenitor (Supplemental Figure S6A). As a result there were only enough control cells to perform a limited Western blot analysis. IPF clonal progeny displayed higher collagen I and α-SMA expression than did control clonal progeny (Supplemental Figure S6B). However, a sufficient number of control clonal progeny were available to perform the zebrafish xenograft assay. In marked contrast to IPF clonal progeny, the clonal progeny of a single control mesenchymal progenitor cell did not form a fibrotic reticulum; engrafted cells were predominantly nonmotile in the zebrafish (Figure 4D, Supplemental Figure S6C, and Supplemental Table S2). These data proved that IPF mesenchymal progenitors can produce progeny manifesting the phenotypic hallmarks of the IPF fibroblast.

IPF Fibrotic Reticulum Contains Mesenchymal Cells Expressing Progenitor Determinants

Next, we sought to determine whether cells with mesenchymal progenitor determinants or their progeny resided in IPF fibrotic lesions by analyzing lung pathological specimens from patients with IPF ($n = 12$) and patient controls ($n = 5$). For this purpose, on the basis of our results and prior knowledge,[47,55] we used SSEA4 expression combined with localization of Oct4 to identify IPF mesenchymal progenitors (SSEA4$^+$/nuclear Oct4$^+$/cytoplasmic Oct4$^-$) and their progeny (SSEA4$^-$/nuclear Oct4$^-$/cytoplasmic Oct4$^+$) in lung pathological specimens from patients with IPF ($n = 12$).

SSEA4$^+$ cells were interspersed throughout the IPF fibrotic reticulum in all 12 specimens examined (Figure 5A and Supplemental Figure S7). To more completely characterize the SSEA4$^+$ cells, we developed a procedure to immunohistochemically double-stain pathological specimens for SSEA4 and Oct4. Our analysis found numerous examples of solitary SSEA4$^+$ cells with nuclear Oct4 scattered throughout the fibrotic reticulum of each specimen

analyzed ($n = 6$) (Figure 5B and Supplemental Figure S8). In addition, fibroblastic foci in all 12 specimens were heavily populated by clusters of SSEA4$^-$ cells that fell into the following three groups: i) a majority population that expressed only cytoplasmic Oct4; ii) some cells expressing both nuclear and cytoplasmic Oct4; and iii) a few cells displaying only nuclear Oct4 (Figure 5C and Supplemental Figure S9, A and B).

Mesenchymal cells comprising fibroblastic foci express high levels of α-SMA.[5] When analyzing serial sections of fibroblastic foci, we found many cells expressing cytoplasmic Oct4 and α-SMA ($n = 4$) (Figure 5D). Thus, a small number of cells with progenitor determinants (SSEA4$^+$/nuclear Oct4$^+$) populated the IPF fibrotic reticulum, accompanied by a larger number of mesenchymal cells with characteristics of their progeny (α-SMA$^+$/SSEA4$^-$/cytoplasmic Oct4$^+$). Of note, relatively intact alveoli adjacent to fibrotic regions did not contain Oct4 immunoreactive cells (Supplemental Figure S9C). The alveolar walls of control lung tissue contained no cells with Oct4 or SSEA4 immunoreactivity (Supplemental Figure S10,

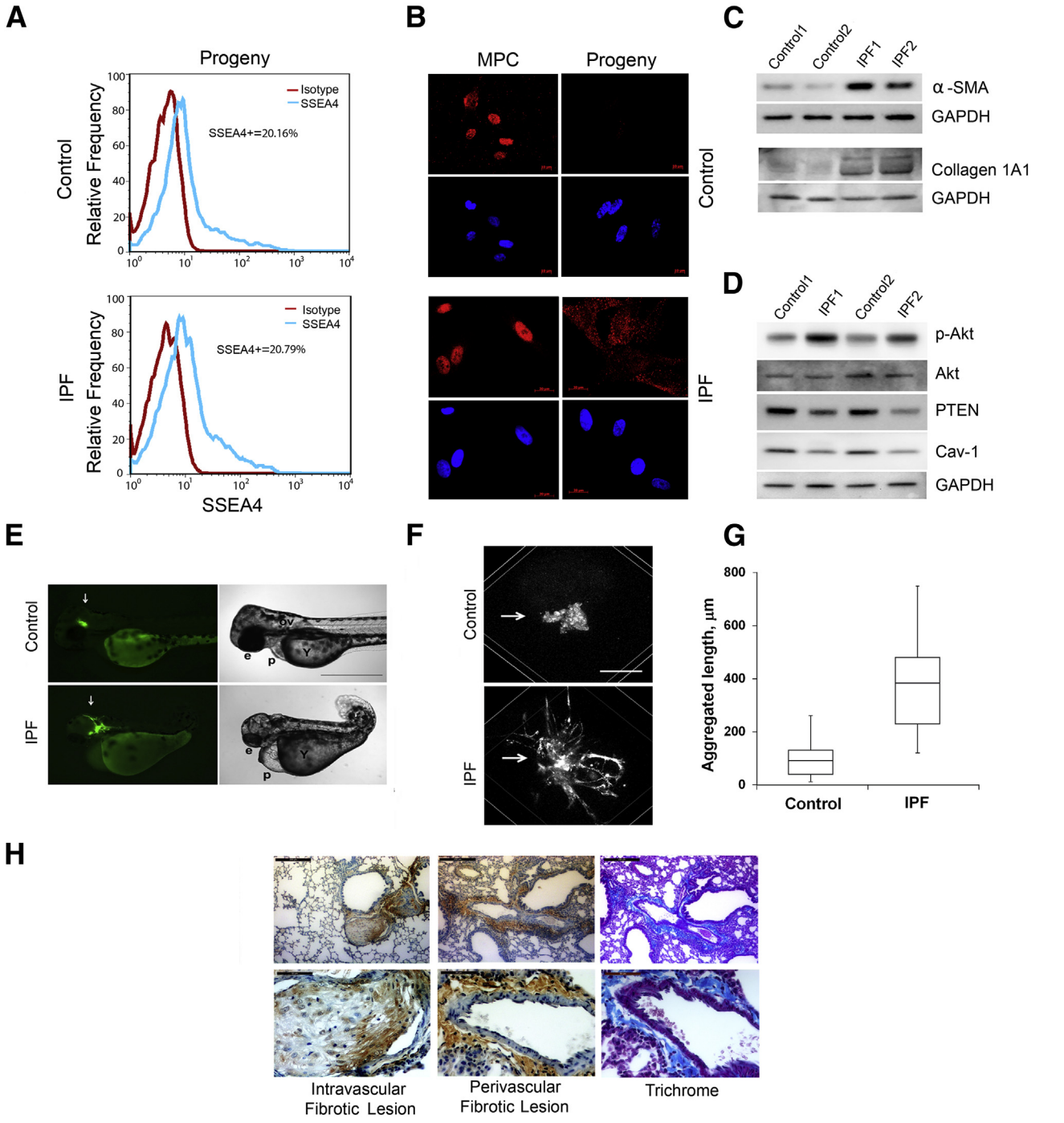

Table 1 Zebrafish Xenograft Data

Cell lines*	Graft-bearing embryos, *N*	Normal embryos, *n* (%)	Abnormal embryos, *n* (%)	Fibrotic reticulum
IPF primary mesenchymal cells†	35	4 (11.4)	31 (88.6)	Yes
IPF MPCs	43	36 (83.7)	7 (16.3)	No
IPF MPC-progeny	65	7 (10.8)	58 (89.2)	Yes
Control primary mesenchymal cells†	48	3 (6.3)	45 (93.7)	No
Control MPCs	15	12 (80)	3 (20)	No
Control MPC-progeny	95	14 (14.7)	81 (85.3)	No

*Data shown are from two IPF cell lines and two control cell lines.
†In accord with our published data.[16]
MPCs, mesenchymal progenitor cells.

A and B). However, SSEA4-expressing cells were observed in small and large airways and vascular structures of control lung tissue (Supplemental Figure S10C). Thus, IPF mesenchymal progenitor cells and cells bearing determinants of their daughter cells populate the fibrotic reticulum in IPF.

Genes and Pathways That Distinguish IPF Mesenchymal Progenitor Cells and Their Progeny from Their Control Counterparts Are Co-Regulated

To determine whether IPF and control progeny displayed disparate patterns of gene expression similar to their progenitors, we defined their steady state mRNA levels genomewide. In accord with their distinct *in vivo* phenotypes, IPF and control progeny displayed significant gene expression differences (Figure 6A). Validation testing of the daughter cell gene expression profiling data set for the same four genes examined in the progenitor data set (*FLT1, MAP3K8, IGF2BP1, YBX1*) confirmed the profiling data for all four genes (Supplemental Figure S11). A heatmap of the 50 most significant genes ($P < 0.002$) indicated that IPF progeny displayed a distinct molecular signature (Figure 6C), and gene set enrichment analysis indicated major differences in many of the same ontologies that distinguish IPF from control progenitors (Supplemental Table S3). To determine whether there was genomewide concordance between IPF mesenchymal progenitor cells and their progeny, all genes that were altered ($P < 0.05$) in both IPF mesenchymal progenitors and IPF progeny relative to their control counterparts were collected. On the basis of the hypothesis that some of the defining gene expression characteristics of IPF mesenchymal progenitors should be retained in their progeny, we analyzed whether these genes were co-regulated (ie, up-regulated in both IPF mesenchymal progenitors and IPF progeny or down-regulated in both IPF mesenchymal progenitors and IPF progeny). Our data indicated a striking degree of co-regulation among the genes that distinguish IPF from control ($P = 1.9 \times 10^{-15}$, Fisher exact test) (Figure 6B and Table 3). Thus, the molecular underpinnings of the IPF fibroblast are reflected by genomewide changes in the transcriptome that can be traced from its cell of origin.

Discussion

The majority fibroblast population derived from the IPF lung manifests a distinct pathological phenotype, but its origin

Figure 3 The progeny of IPF MPCs display IPF fibroblast hallmarks. **A:** SSEA4 expression of progeny by flow cytometry. For reference, shown are isotype controls and a representative SSEA4 expression distribution of MPCs (ie, $SSEA4^+/SSEA1^-$/small cells that have undergone FACS). Data shown are from progeny derived from four independent MPC lines [IPF ($n = 2$), control ($n = 2$)]. **B:** Oct4 localization by immunofluorescence, DAPI to stain nuclei. **C:** α-SMA and collagen I expression. IPF and control progeny were analyzed by Western blot analysis. GAPDH is shown as a loading control. **D:** Akt signaling. IPF and control progeny were released from dishes with trypsin, cultured on 2-mg/mL polymerized collagen matrices for 48 hours, and cell extracts were examined for expression of caveolin-1, phospho-Akt, and PTEN by Western blot analysis. GAPDH is shown as a loading control. **E–G:** The progeny from four independent MPC lines were grafted into zebrafish embryos. Zebrafish xenograft assay (**E**). The progeny of control and IPF progenitors were stained with CFSE, engrafted into zebrafish embryos, and microscopically analyzed in live embryos after 48 hours. Shown are fluorescence (**left panels**) and bright field (**right panels**) images representative of at least 58 embryos per cell line. **Arrows** point to graft location. Graft-related embryonic deformities ranged from severe (microcephaly, microphthalmia, pericardial edema, **upper right panel**) to mild (head lump, **lower right panel**). Embryo orientation in the lateral view was from head to the left. **F:** Zebrafish xenograft assay with three-dimensional reconstruction. Control and IPF progeny were labeled with PKH26 vital dye. Fluorescent grafts were analyzed by single-photon confocal scanning. Shown are representative three-dimensional computer-generated reconstructions of the grafts 48 hours after grafting (**arrows** point to grafts). **G:** Shown is quantification of aggregated length of all processes in IPF and control grafts. **H:** Mouse xenograft assay. The progeny from seven independent MPC lines were injected into the tail vein of mice. Shown are representative images of the lungs (received the progeny of IPF progenitor cells). Human cells were identified with anti-human β_2 microglobulin antibody. Sections shown indicate intravascular and perivascular fibrotic lesions, and trichrome stains of perivascular fibrotic lesions. Not shown here (Supplemental Figure S5) are normal lungs from mice that received the progeny of control progenitors. **G:** Data are expressed as follows: the horizontal line in the middle of each box indicates the median, and the top and bottom borders of the box mark the 75th and 25th percentiles; the whiskers above and below the box mark the 90th and 10th percentiles. $n = 2$ (**A** and **E–G**, IPF and control); $n = 26$ (**G**, IPF grafts); $n = 27$ (**G**, control grafts); $n = 4$ (**H**, IPF); $n = 3$ (**H**, control). $P = 0.001$, IPF grafts versus control grafts (**G**); $P < 0.0001$, composite reticulum length IPF versus control (**G**). Scale bars: 250 μm (**E**); 50 μm (**F**); 200 μm (**H**, **left panels**); 50 μm (**H**, **right panels**). Cav-1, caveolin-1; Collagen 1A1, type I collagen; e, eye; GAPDH, glyceraldehyde-3-phosphate dehydrogenase; MPC, mesenchymal progenitor cell; ov, otic vesicle; p, pericardium; Y, yolk sack.

Table 2 Mouse Xenograft Data

Cell line	Subject	Fibrotic lesions*
IPF 1	Mouse 1	Yes
IPF 1	Mouse 2	Yes
IPF 1	Mouse 3	Yes
IPF 2	Mouse 4	Yes
IPF 3	Mouse 5	Yes
IPF 4	Mouse 6	Yes
Control 1	Mouse 7	No
Control 2	Mouse 8	No
Control 3	Mouse 9	No
Control 3	Mouse 10	No
Control 3	Mouse 11	No

*$P < 0.0022$ compares fibrotic lesions resulting from injection of daughter cells derived from IPF progenitor cells with daughter cells derived from control progenitor cells.

remains unknown.[5] Here, we report the discovery of mesenchymal progenitor cells recovered from the IPF lung that generate fibroblasts displaying the IPF phenotype. We demonstrate that IPF mesenchymal progenitor cells are present in the IPF fibrotic reticulum, can be isolated and cultivated from IPF lungs, and that the daughter cells of these IPF mesenchymal progenitors generate fibrotic lesions when grafted into two model organisms. These findings suggest that the fibrogenic mesenchymal progenitor cells we have identified may be causally implicated in the relentless fibroproliferation characteristic of IPF. Our studies provide the first evidence that pathological mesenchymal progenitor cells can serve as cells of origin for IPF fibroblasts. This finding has major implications in efforts to develop therapeutics to interdict the fibrotic process.

In accord with established protocols, we isolated mesenchymal progenitor cells by FACS from primary cultures of mesenchymal cells by using an antibody to SSEA4, a cell surface protein expressed by stem cells.[42] However, analysis of the sort did not indicate a discrete subpopulation of $SSEA4^+$ cells. Instead, it revealed a gradient of SSEA4-expressing cells. The spectrum ranged from a small subpopulation of cells strongly expressing SSEA4, merging into a distribution of cells displaying a diminishing amount of

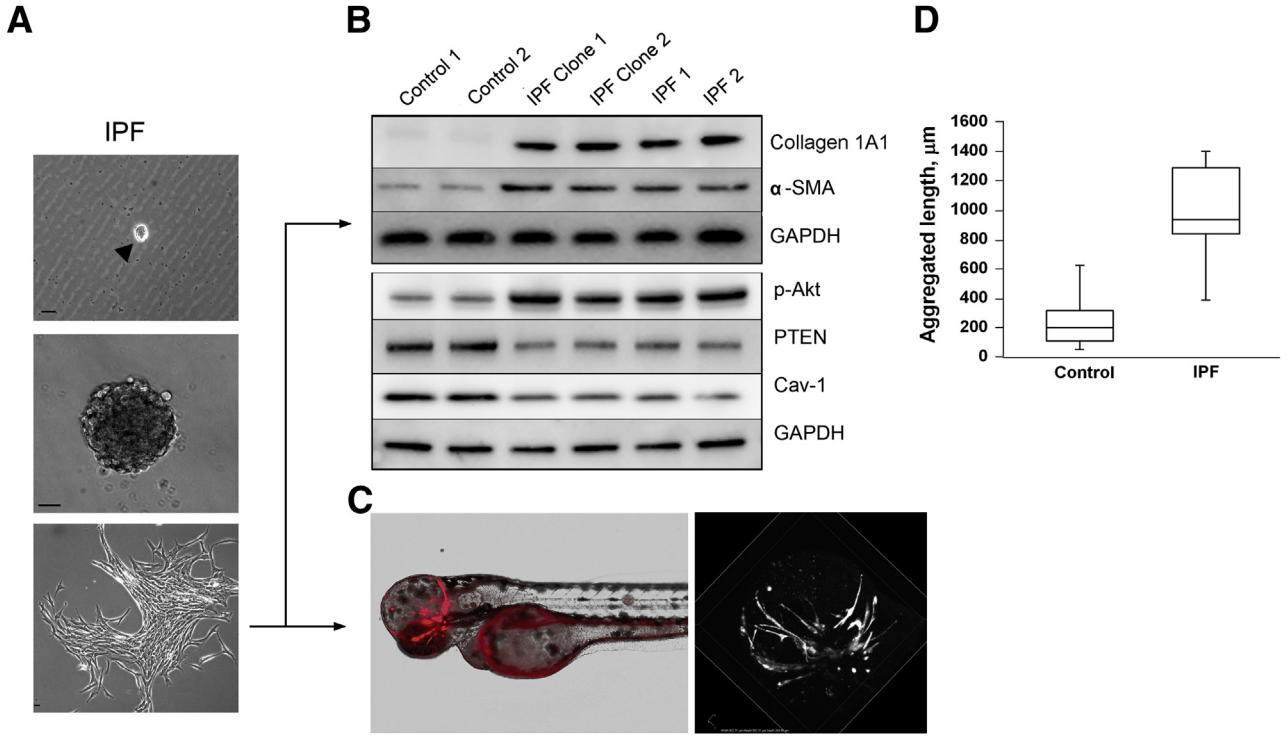

Figure 4 The progeny of a single IPF mesenchymal progenitor cell displays the IPF fibroblast phenotype. **A:** Derivation of progeny from a single progenitor. **Upper panel:** $SSEA4^+$ cells (99% pure) that had undergone FACS were seeded at one cell per well in 96-well dishes coated with methylcellulose and were observed for colony formation. The **arrow** denotes a single SSEA4 expressing IPF mesenchymal progenitor cell (MPC). **Middle panel:** Shown is a phase-contrast image of a colony formed by the progeny of a single progenitor cell. **Bottom panel:** Expansion of the colony on a tissue culture dish. **B:** IPF clonal progeny have the biochemical hallmarks of IPF fibroblasts. Western blots of the progeny of mesenchymal progenitors with each lane representing the clonal progeny of a single progenitor, designated IPF clone 1 (lane 3) and IPF clone 2 (lane 4) for collagen 1A1, α-SMA, GAPDH, p-Akt, PTEN, and Cav-1. Results for two primary control mesenchymal cell lines (designated control 1 and 2; lanes 1 and 2) and two primary IPF mesenchymal cell lines (designated IPF 1 and 2; lanes 5 and 6) are shown as a reference. **C:** IPF clonal progeny form a fibrotic reticulum in zebrafish. An example representative of seven zebrafish embryos grafted with the progeny of a single IPF progenitor. Graft forming a fibrotic reticulum (red) appears in head region with nonspecific autofluorescence outlining the yolk sac (**left panel**). A representative three-dimensional computer-generated reconstruction of the xenograft 48 hours after grafting shows the formation of a fibrotic reticulum (**right panel**). **D:** Quantification of aggregated length of all processes in IPF and control clonal progeny grafts. Data are expressed as follows: the horizontal line in the middle of each box indicates the median, and the top and bottom borders of the box mark the 75th and 25th percentiles; the whiskers above and below the box mark the 90th and 10th percentiles (**D**). $n = 10$ (**D**, IPF grafts); $n = 25$ (**D**, control). $P < 0.001$ (**D**). Scale bars: 10 µm (**A**). Cav-1, caveolin-1; Collagen 1A1, type I collagen; GAPDH, glyceraldehyde-3-phosphate dehydrogenase; p-Akt, phospho-Akt; α-SMA, α-smooth muscle actin.

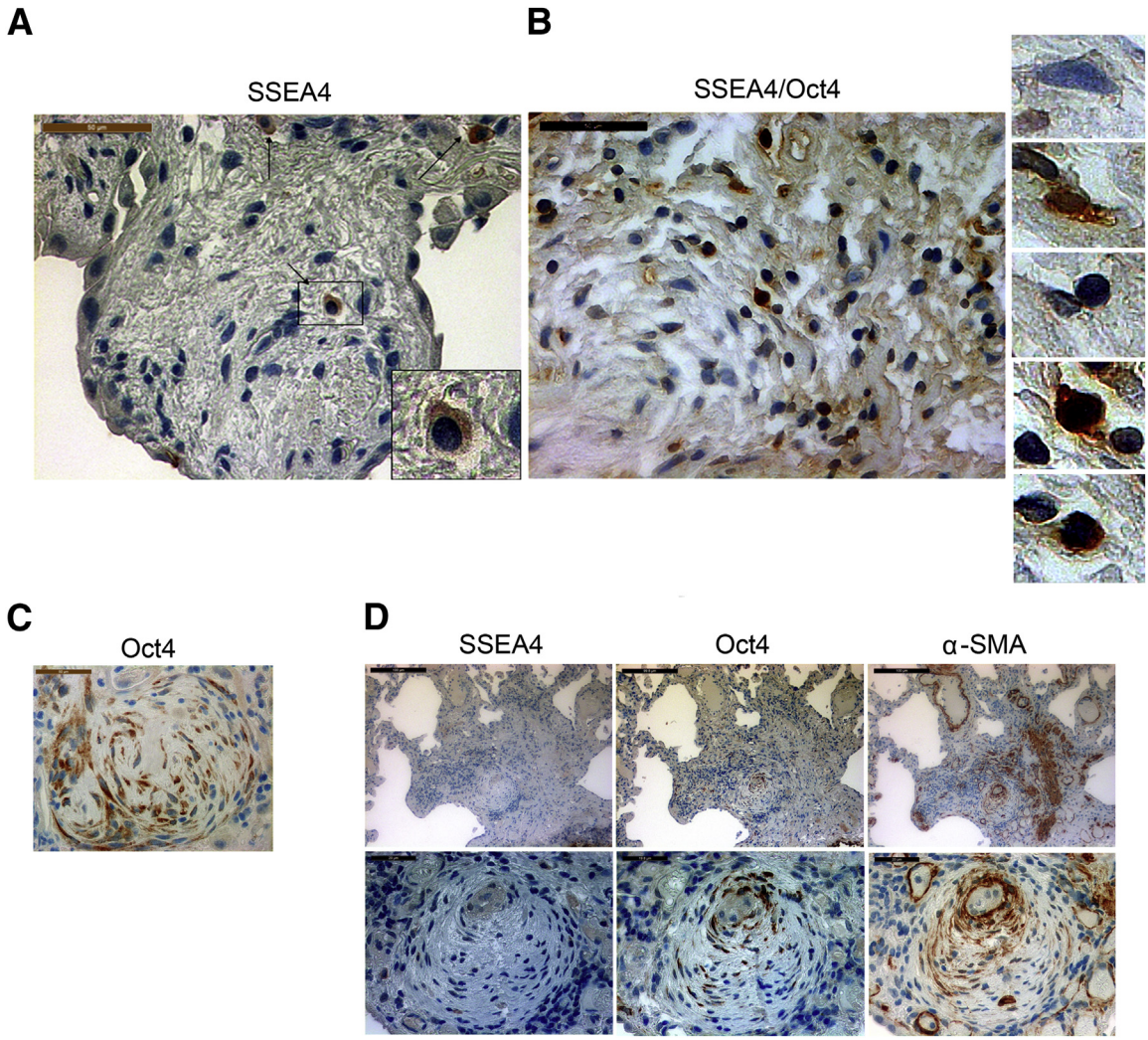

Figure 5 Mesenchymal progenitor cells and their progeny are present in the IPF fibrotic reticulum. **A:** Analysis of IPF lung specimens for cells that express SSEA4, Oct4, and α-SMA. SSEA4-expressing cells in and around the perimeter of an IPF fibroblastic focus. **Arrows** point to SSEA4 expressing cells. The **inset** highlights an SSEA4 immunoreactive cell. **B, left panel:** Double staining for SSEA4 and Oct4 identified SSEA4$^+$ cells with a nuclear Oct4 staining pattern within the IPF fibrotic reticulum. SSEA4 is shown in brown (DAB) and Oct4 in black (DAB/Ni). **Right panels:** High magnification images of cells within the fibroblastic focus shows a nonimmunoreactive cell, a cell immunoreactive for SSEA4 only, a cell immunoreactive for Oct4 only, and two cells immunoreactive for both SSEA4 and Oct4 are shown (top to bottom, respectively). **C:** An IPF fibroblastic focus heavily populated with cells displaying cytoplasmic Oct4. **D:** Serial sections of an IPF fibroblastic focus. Several cells express SSEA4 in and around the focus; however, most cells within the focus do not display SSEA4 immunoreactivity (**left panels**). Cells display cytoplasmic Oct4 and α-smooth muscle actin in a similar distribution (**middle** and **right panels**). $n = 12$ (**A**). Scale bars: 50 μm (**A**–**C**); 100 μm (**D, top left** and **right panels**); 99.8 μm (**D, top middle panel**); 20 μm (**D, bottom left** and **right panels**); 19.8 μm (**D, bottom middle panel**). α-SMA, α-smooth muscle actin.

SSEA4, that in turn merged with a majority population of cells lacking SSEA4 expression. Our studies indicate that the cells strongly expressing SSEA4 also express nuclear Oct4 and share properties with MSCs. As these mesenchymal progenitors propagated and differentiated, their daughter cells lost SSEA4 expression, and Oct4 shifted from a nuclear to cytoplasmic location. Phenotypic analysis of this SSEA4$^-$/nuclear Oct4$^-$/cytoplasmic Oct4$^+$ daughter cell population reveals properties associated with their origin—IPF or control. We interpret these data to indicate that the SSEA4$^-$ population of IPF mesenchymal cells represents a differentiation spectrum that ranges from early generations of progenitor cell progeny up to activated myofibroblasts. It will be important to identify surface determinants to enable accurate classification of these different differentiation states to gain a full understanding of mesenchymal cell population dynamics in the IPF lung.

Although healthy tissues contain MSCs that function to repair tissue after injury,[22,56] and great enthusiasm has been expressed for their therapeutic potential in many diseases, including IPF,[57] there is precedent for mesenchymal progenitors to participate in disease pathogenesis. With the use of animal models of disease, several studies report that normal MSCs and bone marrow progenitor cells can differentiate into fibroblasts that contribute to pathological processes.[56,58,59] Normal MSCs can also produce transforming growth factor-β and Wnt proteins that can stimulate fibroblast proliferation.[60] In human disease, bone marrow MSCs from patients

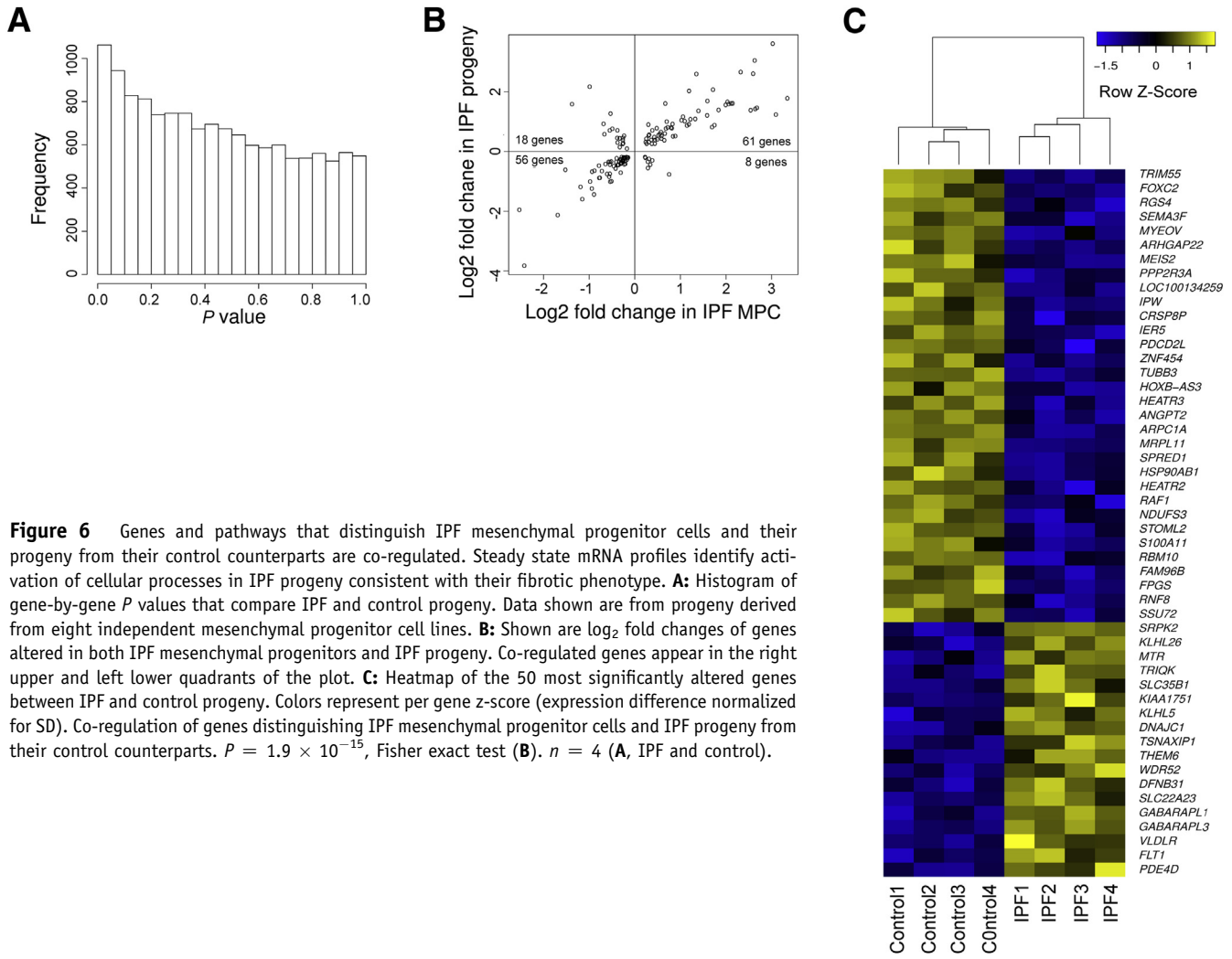

Figure 6 Genes and pathways that distinguish IPF mesenchymal progenitor cells and their progeny from their control counterparts are co-regulated. Steady state mRNA profiles identify activation of cellular processes in IPF progeny consistent with their fibrotic phenotype. **A:** Histogram of gene-by-gene *P* values that compare IPF and control progeny. Data shown are from progeny derived from eight independent mesenchymal progenitor cell lines. **B:** Shown are $\log_2$ fold changes of genes altered in both IPF mesenchymal progenitors and IPF progeny. Co-regulated genes appear in the right upper and left lower quadrants of the plot. **C:** Heatmap of the 50 most significantly altered genes between IPF and control progeny. Colors represent per gene z-score (expression difference normalized for SD). Co-regulation of genes distinguishing IPF mesenchymal progenitor cells and IPF progeny from their control counterparts. $P = 1.9 \times 10^{-15}$, Fisher exact test (**B**). $n = 4$ (**A**, IPF and control).

with multiple myeloma manifest durable abnormalities that promote malignant cell maintenance and progression,[61] and mesenchymal progenitors can be identified at sites of chronic lung allograft rejection.[33,34] Consistently, we identify pathological mesenchymal progenitor cells in the IPF lung that generate progeny that manifest the IPF fibroblast phenotype. However, it is important to note that our data do not reveal the origin of the pathological IPF MPCs we have identified; currently, we lack the tools to determine whether they are derived from normal resident lung MSCs, bone marrow MSCs, a pathological de-differentiation event, or another source. It also remains to be determined whether the pathway we have discovered in IPF from pathological mesenchymal progenitors to diseased fibroblasts represents a more general paradigm for progressive fibrosis in other fibrotic lung disorders or for fibrosis of other organs.

Our study does not directly address the mechanisms leading to the stable acquisition of a pathological state by IPF mesenchymal progenitors or their progeny; however, an elegant study that examined the ability of extracellular matrix to durably shape fibroblast phenotype provides insight into how this might occur.[62] In that report, lung fibroblasts cultured on stiff matrices become activated and continue to express an activated phenotype even when returned to pliable matrices, providing proof of concept for durable reprogramming of mesenchymal cells on the basis of the mechanics of the matrix microenvironment. This finding raises the possibility that a fibrotic extracellular matrix as is found in IPF could stably skew the phenotype of mesenchymal progenitors and their progeny.

To our knowledge, our study is the first to show that mesenchymal progenitor cells derived from a naturally occurring human fibrotic organ can generate progeny with the biological properties and molecular hallmarks of fibrotic fibroblasts. Transcriptional profiling revealed a distinct gene expression profile that distinguished IPF mesenchymal progenitor cells and their daughter cells from controls. Consistent with the idea that the hallmarks of the IPF fibroblast have their roots in pathological mesenchymal progenitor cells, we observed striking concordance among the genes and pathways that were significantly altered in both IPF mesenchymal progenitor cells and their progeny relative to controls.

Table 3 List of Co-Regulated Disease-Associated Genes in IPF Mesenchymal Progenitors and IPF Progeny

Genes co-regulated up in both IPF MPC and progeny				Genes co-regulated down in both IPF MPC and progeny			
1	*FAM225B*	32	*A4GALT*	1	*SNORD116-20*	32	*LOC440563*
2	*MICA*	33	*SNRK*	2	*MIR1244-1*	33	*NDP*
3	*LHFP*	34	*ETNK2*	3	*PQBP1*	34	*NDUFS3*
4	*GPNMB*	35	*PRKACB*	4	*RPP38*	35	*NEFH*
5	*RAB31*	36	*TMEM184C*	5	*IGF2BP1*	36	*YBX1*
6	*BVES*	37	*MCTP2*	6	*WDR6*	37	*MBIP*
7	*FICD*	38	*PSEN1*	7	*RPL35*	38	*ATP6V1G2*
8	*CYGB*	39	*PLSCR4*	8	*INO80C*	39	*GNB1L*
9	*GJD3*	40	*PTGFRN*	9	*NUDT10*	40	*FOXRED1*
10	*MAP3K8*	41	*SERINC1*	10	*EEF1B2*	41	*DDX28*
11	*EDNRB*	42	*PTPRM*	11	*FBL*	42	*DANCR*
12	*EIF2C4*	43	*SSR4P1*	12	*FAU*	43	*MRPS26*
13	*A2M*	44	*TNFSF4*	13	*DNAJC8*	44	*MRPL11*
14	*EPAS1*	45	*OSGIN2*	14	*EXOSC7*	45	*MRPL9*
15	*STOM*	46	*BEST1*	15	*PPRC1*	46	*SNRPA*
16	*FLT1*	47	*TMEM204*	16	*PES1*	47	*SRP68*
17	*SASH1*	48	*GALNT12*	17	*RPL36*	48	*SNORA24*
18	*GFRA1*	49	*CCDC68*	18	*ODZ4*	49	*SNORA40*
19	*ZADH2*	50	*ZNF611*	19	*SNORD52*	50	*C1QBP*
20	*GPR37*	51	*TMTC1*	20	*PRPF19*	51	*C11orf83*
21	*FAM225A*	52	*TM2D1*	21	*GNAZ*	52	*FSD1*
22	*OSTM1*	53	*SGIP1*	22	*ZNF454*	53	*PRR3*
23	*TRHDE*	54	*ARHGAP5-AS1*	23	*CHMP4A*	54	*TUBB1*
24	*ICAM1*	55	*RGS9*	24	*HNRNPC*	55	*SYNJ2*
25	*ACER2*	56	*CABLES1*	25	*B4GALNT4*	56	*WDR85*
26	*NCKAP5*	57	*ACVRL1*	26	*IMPDH2*		
27	*GVINP1*	58	*SCARB2*	27	*IPW*		
28	*RND3*	59	*KIAA0247*	28	*RNF138P1*		
29	*PPAPDC2*	60	*GAB2*	29	*KIF5A*		
30	*MITF*	61	*CLEC2B*	30	*C1orf31*		
31	*NQO2*			31	*ZNF880*		

Moreover, we found that most of these genes and pathways were co-regulated. Thus, our data indicate that IPF mesenchymal progenitor cells display a pathological gene expression pattern and provide initial mechanistic insight into gene pathways that define the IPF phenotype. However, we recognize that this is only the first step. In a disease process as complex as IPF, unraveling the detailed mechanism(s) leading to the genesis of IPF mesenchymal progenitor cells and their differentiation to IPF fibroblasts will likely be unveiled slowly and systematically over many years.

Progressive scarring of the heart, blood vessels, lung, liver, kidney, and brain leads to millions of deaths each year worldwide. Despite decades of intensive investigation, the origin of the fibroblasts that mediate fibrotic organ destruction remained unknown. Several recent publications that used state-of-the-art lineage tracing technology to examine the origin of fibrosis-generating fibroblasts after injury in model organisms have reached definitive, but different conclusions.[63–67] What has been definitively established in a mouse model is that several different stromal populations can contribute to lung fibrogenesis.[67] A lingering problem in this field has been the paucity of direct knowledge about human organ fibrosis. Here, we report the discovery and molecular characterization of mesenchymal progenitor cells, derived from a human fibrotic organ, that are capable of generating daughter cells that have an activated phenotype and autonomously form a fibrotic reticulum *in vivo*. If confirmed by other investigators, our discovery provides strong impetus for a therapeutic paradigm shift focused on developing approaches that target fibrogenic mesenchymal progenitor cells before they generate fibrogenic fibroblasts that mediate organ failure.

Acknowledgments

We thank Dr. Dan Kaufman (Stem Cell Institute, University of Minnesota, Minneapolis, MN) for Oct4, Nanog, and Sox2 PCR primers; iPS cells; and for technical advice; Dr. Angela Panoskaltsis-Mortari (University of Minnesota) for technical advice; the Flow Cytometry Core Facility of the Masonic Cancer Center, a comprehensive cancer center designated by the National Cancer Institute; and University of Minnesota Core Facilities: the Biomedical Genomics Center; The Minnesota Supercomputing Institute; and BIONET for technical support.

Supplemental Data

Supplemental material for this article can be found at *http://dx.doi.org/10.1016/j.ajpath.2014.01.012*.

References

1. Wynn TA, Ramalingam TR: Mechanisms of fibrosis: therapeutic translation for fibrotic disease. Nat Med 2012, 18:1028–1040
2. Fernandez IE, Eickelberg O: New cellular and molecular mechanisms of lung injury and fibrosis in idiopathic pulmonary fibrosis. Lancet 2012, 380:680–688
3. King TE Jr, Pardo A, Selman M: Idiopathic pulmonary fibrosis. Lancet 2011, 378:1949–1961
4. Noble PW: Idiopathic pulmonary fibrosis: natural history and prognosis. Clin Chest Med 2006, 27(1 suppl 1):S11–S16. v
5. Noble PW, Barkauskas CE, Jiang D: Pulmonary fibrosis: patterns and perpetrators. J Clin Invest 2012, 122:2756–2762
6. Raghu G, Weycker D, Edelsberg J, Bradford WZ, Oster G: Incidence and prevalence of idiopathic pulmonary fibrosis. Am J Respir Crit Care Med 2006, 174:810–816
7. King TE, Costabel U, Cordier JF, DoPico GA, DuBois RM, Lynch D, Lynch III JP, Myers J, Panos R, Raghu G, Schwartz D, Smith CM: American Thoracic Society. Idiopathic pulmonary fibrosis: diagnosis and treatment. International consensus statement. American Thoracic Society (ATS), and the European Respiratory Society (ERS). Am J Respir Crit Care Med 2000, 161:646–664
8. Travis WD, King TE, Bateman ED, Lynch DA, Capron F, Center D, Colby TV, Cordier JF, DuBois RM, Galvin J, Grenier P, Hansell DM, Hunninghake GW, Kitaichi M, Muller NL, Myers JL, Nagai S, Nicholson A, Raghu G, Wallaert B. American Thoracic Society; European Respiratory Society: American Thoracic Society/European Respiratory Society International Multidisciplinary Consensus Classification of the Idiopathic Interstitial Pneumonias. This joint statement of the American Thoracic Society (ATS), and the European Respiratory Society (ERS) was adopted by the ATS board of directors, June 2001 and by the ERS Executive Committee, June 2001. Am J Respir Crit Care Med 2002, 165:277–304
9. Cool CD, Groshong SD, Rai PR, Henson PM, Stewart JS, Brown KK: Fibroblast foci are not discrete sites of lung injury or repair: the fibroblast reticulum. Am J Respir Crit Care Med 2006, 174:654–658
10. Kuhn C, McDonald JA: The roles of the myofibroblast in idiopathic pulmonary fibrosis. Ultrastructural and immunohistochemical features of sites of active extracellular matrix synthesis. Am J Pathol 1991, 138:1257–1265
11. Noble PW, Homer RJ: Idiopathic pulmonary fibrosis: new insights into pathogenesis. Clin Chest Med 2004, 25:749–758, vii
12. Selman M, King TE, Pardo A; American Thoracic Society; European Respiratory Society; American College of Chest Physicians: Idiopathic pulmonary fibrosis: prevailing and evolving hypotheses about its pathogenesis and implications for therapy. Ann Intern Med 2001, 134:136–151
13. Xia H, Diebold D, Nho R, Perlman D, Kleidon J, Kahm J, Avdulov S, Peterson M, Nerva J, Bitterman P, Henke C: Pathological integrin signaling enhances proliferation of primary lung fibroblasts from patients with idiopathic pulmonary fibrosis. J Exp Med 2008, 205: 1659–1672
14. Xia H, Khalil W, Kahm J, Jessurun J, Kleidon J, Henke CA: Pathologic caveolin-1 regulation of PTEN in idiopathic pulmonary fibrosis. Am J Pathol 2010, 176:2626–2637
15. Xia H, Seeman J, Hong J, Hergert P, Bodem V, Jessurun J, Smith K, Nho R, Kahm J, Gaillard P, Henke C: Low alpha(2)beta(1) integrin function enhances the proliferation of fibroblasts from patients with idiopathic pulmonary fibrosis by activation of the beta-catenin pathway. Am J Pathol 2012, 181:222–233
16. Benyumov AO, Hergert P, Herrera J, Peterson M, Henke C, Bitterman PB: A novel zebrafish embryo xenotransplantation model to study primary human fibroblast motility in health and disease. Zebrafish 2012, 9:38–43
17. Pierce EM, Carpenter K, Jakubzick C, Kunkel SL, Flaherty KR, Martinez FJ, Hogaboam CM: Therapeutic targeting of CC ligand 21 or CC chemokine receptor 7 abrogates pulmonary fibrosis induced by the adoptive transfer of human pulmonary fibroblasts to immunodeficient mice. Am J Pathol 2007, 170:1152–1164
18. Giangreco A, Reynolds SD, Stripp BR: Terminal bronchioles harbor a unique airway stem cell population that localizes to the bronchoalveolar duct junction. Am J Pathol 2002, 161:173–182
19. Kajstura J, Rota M, Hall SR, Hosoda T, D'Amario D, Sanada F, Zheng H, Ogorek B, Rondon-Clavo C, Ferreira-Martins J, Matsuda A, Arranto C, Goichberg P, Giordano G, Haley KJ, Bardelli S, Rayatzadeh H, Liu X, Quaini F, Liao R, Leri A, Perrella MA, Loscalzo J, Anversa P: Evidence for human lung stem cells. N Engl J Med 2011, 364:1795–1806
20. Kim CF, Jackson EL, Woolfenden AE, Lawrence S, Babar I, Vogel S, Crowley D, Bronson RT, Jacks T: Identification of bronchioalveolar stem cells in normal lung and lung cancer. Cell 2005, 121:823–835
21. Majka SM, Beutz MA, Hagen M, Izzo AA, Voelkel N, Helm KM: Identification of novel resident pulmonary stem cells: form and function of the lung side population. Stem Cells 2005, 23:1073–1081
22. Ortiz LA, Gambelli F, McBride C, Gaupp D, Baddoo M, Kaminski N, Phinney DG: Mesenchymal stem cell engraftment in lung is enhanced in response to bleomycin exposure and ameliorates its fibrotic effects. Proc Natl Acad Sci U S A 2003, 100:8407–8411
23. Stripp BR, Shapiro SD: Stem cells in lung disease, repair, and the potential for therapeutic interventions: state-of-the-art and future challenges. Am J Respir Cell Mol Biol 2006, 34:517–518
24. Summer R, Fitzsimmons K, Dwyer D, Murphy J, Fine A: Isolation of an adult mouse lung mesenchymal progenitor cell population. Am J Respir Cell Mol Biol 2007, 37:152–159
25. Summer R, Kotton DN, Liang S, Fitzsimmons K, Sun X, Fine A: Embryonic lung side population cells are hematopoietic and vascular precursors. Am J Respir Cell Mol Biol 2005, 33:32–40
26. Weiss DJ, Kolls JK, Ortiz LA, Panoskaltsis-Mortari A, Prockop DJ: Stem cells and cell therapies in lung biology and lung diseases. Proc Am Thorac Soc 2008, 5:637–667
27. Al-Hajj M, Wicha MS, Benito-Hernandez A, Morrison SJ, Clarke MF: Prospective identification of tumorigenic breast cancer cells. Proc Natl Acad Sci U S A 2003, 100:3983–3988
28. Bonnet D, Dick JE: Human acute myeloid leukemia is organized as a hierarchy that originates from a primitive hematopoietic cell. Nat Med 1997, 3:730–737
29. Clevers H: The cancer stem cell: premises, promises and challenges. Nat Med 2011, 17:313–319
30. Mani SA, Guo W, Liao MJ, Eaton EN, Ayyanan A, Zhou AY, Brooks M, Reinhard F, Zhang CC, Shipitsin M, Campbell LL, Polyak K, Brisken C, Yang J, Weinberg RA: The epithelial-mesenchymal transition generates cells with properties of stem cells. Cell 2008, 133:704–715
31. Reya T, Morrison SJ, Clarke MF, Weissman IL: Stem cells, cancer, and cancer stem cells. Nature 2001, 414:105–111
32. Wu C, Amini-Nik S, Nadesan P, Stanford WL, Alman BA: Aggressive fibromatosis (desmoid tumor) is derived from mesenchymal progenitor cells. Cancer Res 2010, 70:7690–7698
33. Badri L, Murray S, Liu LX, Walker NM, Flint A, Wadhwa A, Chan KM, Toews GB, Pinsky DJ, Martinez FJ, Lama VN: Mesenchymal stromal cells in bronchoalveolar lavage as predictors of bronchiolitis obliterans syndrome. Am J Respir Crit Care Med 2011, 183:1062–1070
34. Lama VN, Smith L, Badri L, Flint A, Andrei AC, Murray S, Wang Z, Liao H, Toews GB, Krebsbach PH, Peters-Golden M, Pinsky DJ, Martinez FJ, Thannickal VJ: Evidence for tissue-resident mesenchymal stem cells in human adult lung from studies of transplanted allografts. J Clin Invest 2007, 117:989–996

35. Chen B, Polunovsky V, White J, Blazar B, Nakhleh R, Jessurun J, Peterson M, Bitterman P: Mesenchymal cells isolated after acute lung injury manifest an enhanced proliferative phenotype. J Clin Invest 1992, 90:1778–1785
36. Larsson O, Diebold D, Fan D, Peterson M, Nho RS, Bitterman PB, Henke CA: Fibrotic myofibroblasts manifest genome-wide derangements of translational control. PLoS One 2008, 3:e3220
37. Rijlaarsdam MA, van Herk HA, Gillis AJ, Stoop H, Jenster G, Martens J, van Leenders GJ, Dinjens W, Hoogland AM, Timmermans M, Looijenga LH: Specific detection of OCT3/4 isoform A/B/B1 expression in solid (germ cell) tumours and cell lines: confirmation of OCT3/4 specificity for germ cell tumours. Br J Cancer 2011, 105:854–863
38. Wright GW, Simon RM: A random variance model for detection of differential gene expression in small microarray experiments. Bioinformatics 2003, 19:2448–2455
39. Luo W, Friedman MS, Shedden K, Hankenson KD, Woolf PJ: GAGE: generally applicable gene set enrichment for pathway analysis. BMC Bioinformatics 2009, 10:161
40. Harris MA, Deegan JI, Ireland A, Lomax J, Ashburner M, Tweedie S, Carbon S, Lewis S, Mungall C, Day-Richter J, Eilbeck K, Blake JA, Bult C, Diehl AD, Dolan M, Drabkin H, Eppig JT, Hill DP, Ni L, Ringwald M, Balakrishnan R, Binkley G, Cherry JM, Christie KR, Costanzo MC, Dong Q, Engel SR, Fisk DG, Hirschman JE, Hitz BC, Hong EL, Krieger CJ, Miyasato SR, Hash RS, Park J, Skrzpek MS, et al. Gene Ontology Consortium: The Gene Ontology project in 2008. Nucleic Acids Res 2008, 36:D440–D444
41. Larsson O, Perlman DM, Fan D, Reilly CS, Peterson M, Dahlgren C, Liang Z, Li S, Polunovsky VA, Wahlestedt C, Bitterman PB: Apoptosis resistance downstream of eIF4E: posttranscriptional activation of an anti-apoptotic transcript carrying a consensus hairpin structure. Nucleic Acids Res 2006, 34:4375–4386
42. Gang EJ, Bosnakovski D, Figueiredo CA, Visser JW, Perlingeiro RC: SSEA-4 identifies mesenchymal stem cells from bone marrow. Blood 2007, 109:1743–1751
43. Dominici M, Le Blanc K, Mueller I, Slaper-Cortenbach I, Marini F, Krause D, Deans R, Keating A, Prockop D, Horwitz E: Minimal criteria for defining multipotent mesenchymal stromal cells. The International Society for Cellular Therapy position statement. Cytotherapy 2006, 8:315–317
44. Moore BB, Kolodsick JE, Thannickal VJ, Cooke K, Moore TA, Hogaboam C, Wilke CA, Toews GB: CCR2-mediated recruitment of fibrocytes to the alveolar space after fibrotic injury. Am J Pathol 2005, 166:675–684
45. Short B, Brouard N, Occhiodoro-Scott T, Ramakrishnan A, Simmons PJ: Mesenchymal stem cells. Arch Med Res 2003, 34:565–571
46. Ramos C, Montano M, Garcia-Alvarez J, Ruiz V, Uhal BD, Selman M, Pardo A: Fibroblasts from idiopathic pulmonary fibrosis and normal lungs differ in growth rate, apoptosis, and tissue inhibitor of metalloproteinases expression. Am J Respir Cell Mol Biol 2001, 24:591–598
47. Ferro F, Spelat R, D'Aurizio F, Puppato E, Pandolfi M, Beltrami AP, Cesselli D, Falini G, Beltrami CA, Curcio F: Dental pulp stem cells differentiation reveals new insights in Oct4A dynamics. PLoS One 2012, 7:e41774
48. Estrada J, Li P, Mir B: Multiorgan engraftment of human somatic cells in swine foetuses after intra-blastocyst transplantation. Reprod Domest Anim 2011, 46:630–635
49. Harder F, Henschler R, Junghahn I, Lamers MC, Muller AM: Human hematopoiesis in murine embryos after injecting human cord blood-derived hematopoietic stem cells into murine blastocysts. Blood 2002, 99:719–721
50. Harder F, Kirchhof N, Petrovic S, Schmittwolf C, Durr M, Muller AM: Developmental potentials of hematopoietic and neural stem cells following injection into pre-implantation blastocysts. Ann Hematol 2002, 81(suppl 2):S20–S21
51. Harder F, Kirchhof N, Petrovic S, Wiese S, Muller AM: Erythroid-like cells from neural stem cells injected into blastocysts. Exp Hematol 2004, 32:673–682
52. Parameswaran V, Laize V, Gavaia PJ, Leonor Cancela M: ESSA1 embryonic stem like cells from gilthead seabream: a new tool to study mesenchymal cell lineage differentiation in fish. Differentiation 2012, 84:240–251
53. Prelle K, Zink N, Wolf E: Pluripotent stem cells–model of embryonic development, tool for gene targeting, and basis of cell therapy. Anat Histol Embryol 2002, 31:169–186
54. Siqueira da Fonseca SA, Abdelmassih S, de Mello Cintra Lavagnolli T, Serafim RC, Clemente Santos EJ, Mota Mendes C, de Souza Pereira V, Ambrosio CE, Miglino MA, Visintin JA, Abdelmassih R, Kerkis A, Kerkis I: Human immature dental pulp stem cells' contribution to developing mouse embryos: production of human/mouse preterm chimaeras. Cell Prolif 2009, 42:132–140
55. Lin Y, Yang Y, Li W, Chen Q, Li J, Pan X, Zhou L, Liu C, Chen C, He J, Cao H, Yao H, Zheng L, Xu X, Xia Z, Ren J, Xiao L, Li L, Shen B, Zhou H, Wang YJ: Reciprocal regulation of Akt and Oct4 promotes the self-renewal and survival of embryonal carcinoma cells. Mol Cell 2012, 48:627–640
56. Lee CH, Shah B, Moioli EK, Mao JJ: CTGF directs fibroblast differentiation from human mesenchymal stem/stromal cells and defines connective tissue healing in a rodent injury model. J Clin Invest 2010, 120:3340–3349
57. Toonkel RL, Hare JM, Matthay MA, Glassberg MK: Mesenchymal stem cells and idiopathic pulmonary fibrosis. Potential for clinical testing. Am J Respir Crit Care Med 2013, 188:133–140
58. Sopel MJ, Rosin NL, Lee TD, Legare JF: Myocardial fibrosis in response to Angiotensin II is preceded by the recruitment of mesenchymal progenitor cells. Lab Invest 2011, 91:565–578
59. Spaeth EL, Dembinski JL, Sasser AK, Watson K, Klopp A, Hall B, Andreeff M, Marini F: Mesenchymal stem cell transition to tumor-associated fibroblasts contributes to fibrovascular network expansion and tumor progression. PLoS One 2009, 4:e4992
60. Salazar KD, Lankford SM, Brody AR: Mesenchymal stem cells produce Wnt isoforms and TGF-beta1 that mediate proliferation and procollagen expression by lung fibroblasts. Am J Physiol Lung Cell Mol Physiol 2009, 297:L1002–L1011
61. Reagan MR, Ghobrial IM: Multiple myeloma mesenchymal stem cells: characterization, origin, and tumor-promoting effects. Clin Cancer Res 2012, 18:342–349
62. Balestrini JL, Chaudhry S, Sarrazy V, Koehler A, Hinz B: The mechanical memory of lung myofibroblasts. Integr Biol (Camb) 2012, 4:410–421
63. Hashimoto N, Jin H, Liu T, Chensue SW, Phan SH: Bone marrow-derived progenitor cells in pulmonary fibrosis. J Clin Invest 2004, 113:243–252
64. Humphreys BD, Lin SL, Kobayashi A, Hudson TE, Nowlin BT, Bonventre JV, Valerius MT, McMahon AP, Duffield JS: Fate tracing reveals the pericyte and not epithelial origin of myofibroblasts in kidney fibrosis. Am J Pathol 2010, 176:85–97
65. Kim KK, Kugler MC, Wolters PJ, Robillard L, Galvez MG, Brumwell AN, Sheppard D, Chapman HA: Alveolar epithelial cell mesenchymal transition develops in vivo during pulmonary fibrosis and is regulated by the extracellular matrix. Proc Natl Acad Sci U S A 2006, 103:13180–13185
66. Moeller A, Gilpin SE, Ask K, Cox G, Cook D, Gauldie J, Margetts PJ, Farkas L, Dobranowski J, Boylan C, O'Byrne PM, Strieter RM, Kolb M: Circulating fibrocytes are an indicator of poor prognosis in idiopathic pulmonary fibrosis. Am J Respir Crit Care Med 2009, 179:588–594
67. Rock JR, Barkauskas CE, Cronce MJ, Xue Y, Harris JR, Liang J, Noble PW, Hogan BL: Multiple stromal populations contribute to pulmonary fibrosis without evidence for epithelial to mesenchymal transition. Proc Natl Acad Sci U S A 2011, 108:E1475–E1483